Evolution of the Telencephalon Anterior-Posterior Patterning by Core Endogenous Network Bifurcation

Chen Sun[1#], Mengchao Yao[1#], Ruiqi Xiong[1], Yang Su[1], Binglin Zhu[1], Xile Zhang[1], Ping Ao[2*]

[1.] Shanghai Center for Quantitative Life Sciences and Physics Department, Shanghai University, Shanghai, China;

[2.] Sichuan University, Chengdu, Sichuan Province, China.

# These authors contributed equally to this work.

***Corresponding Authors:**

Ping Ao: Sichuan University, Chengdu, Sichuan Province, China

E-mail: aoping@sjtu.edu.cn

Abstract

How did the complex structure of telencephalon evolve? Existing explanations are based on phenomena and lack the first principle. The Darwinian dynamics and endogenous network theory established decades ago provides a mathematical and theoretical framework of a dynamical structure and a general constitutive structure for theory-experiment coupling separately for answering this question from the first principle perspective. By revisiting a gene network that explains the anterior-posterior patterning of the vertebrate telencephalon, we found that with the increase of the cooperative effect in this network, the fixed points gradually evolve, accompanied by the occurrence of two bifurcations. The dynamic behavior of this network consists of the knowledge obtained from experiments on telencephalon evolution. Our work drew an answer quantitatively of how the telencephalon anterior-posterior patterning evolved from the pre-vertebrate chordate to the vertebrate and gave a series of verifiable predictions in a first principle manner.

Keywords: telencephalon, evolution, gene regulatory network, endogenous network theory, nonlinear process

Introduction

As the material basis of cognitive abilities, the telencephalon results from hundreds of millions of years of evolution(Briscoe & Ragsdale, 2019; Chakraborty & Jarvis, 2015; Holland, 2015). A series of events, like genome duplication and new genes emergence(Kaessmann, 2010; Putnam et al., 2008), core gene network interconnectivity increasing(Gil-Gálvez et al., 2022), neuropathway duplication(Chakraborty & Jarvis, 2015), were discovered, providing phenomenological explanations for how the complex structure of the telencephalon has evolved to this day. But like research on the celestial motion before the introduction of Newtonian mechanics, these phenomena-based explanations lack the fundamental core: the first principle.

Recently, some researchers also worried that researches in life science pay more attention on the experiment itself than the theory-experiment coupling(MacArthur, 2023; Nurse, 2021; Smaldino, 2019); or even had a circling back sensation, at least in cancer research, after half a century of the journey(Weinberg, 2014). Indeed, the phenomena of life are full of complexity, and the complexity science itself is still a newborn one. The discovery of a first principle in life is bound to be difficult. Nonetheless, there were fruits born in this “circle”. Decades after the introduction of Boolean dynamics into the gene network(Kauffman, 1969; Toulouse et al., 2005), the analysis of the dynamical structure of the hydrogen model in life science: the phage-λ gene switch(ZHU et al., 2004), provided an example of application of a general law alone with the mathematical framework for the evolution dynamics(P. Ao, 2005; Kwon et al., 2005). Following this footpath, a theory provides the general constitutive structures of evolution dynamics on the gene network level, the endogenous network theory(Ping Ao et al., 2008) was established years after the postulation of the system biology(Hood, 2003), unifies the gene network dynamics and the landscape concept raised by Wright and Waddington, allowing the qualitative and quantitative comparisons between theories and experiments(Ping Ao, 2021; Prokop, 2022). Under these theoretical sets, a series of efforts were made to address questions on cancer and development(Yuan et al., 2017). Now we may have enough mathematical and theoretical framework as well as the knowledge obtained from experiments

to address the question of how our brain evolved at the gene network dynamics level in a first principle way.

In this work, the attempt was made by revisiting a pre-constructed model(Giacomantonio & Goodhill, 2010, 2014; Goodhill, 2018) of telencephalon anterior-posterior patterning in vertebrates containing 5 nodes and 10 edges, demonstrated that the dynamic behavior of such a relatively small network is necessary to draw an answer under the mathematical and theoretical framework mentioned above.

Results

A coarse-grained core endogenous network for telencephalon already exists

A Boolean 5-node network has been constructed, which sufficiently reproduced the experimentally observed gradients of anterior-posterior patterning of early cortical development in mammals(Giacomantonio & Goodhill, 2010; Goodhill, 2018). From the perspective of data fitting, the existing experimental data were not sufficient to uniquely specify interactions of a base network. And if such a base network exists, how the latent factors regulate the base network is not clear(Giacomantonio & Goodhill, 2010, 2014; Goodhill, 2018).

But in the other way, Giacomantonio and Goodhill have constructed a network with robust dynamic behavior, which is exactly one of the most important features of the “backbone”, or say, the “core” structure of an endogenous network shaped by evolution that we argued in 2008, one of the others is being conserved among species during evolution(Ping Ao et al., 2008; Yuan et al., 2017). We found ortholog exists in amphioxus, one of the closest living vertebrate relatives that diverged from the vertebrate lineage around 550 million years ago, of all 5 genes(Marlétaz et al., 2018; Putnam et al., 2008; Takatori et al., 2008) in this network. Nevertheless, Benito-Gutiérrez *et al.* discovered the resemblance of the expression pattern between mature amphioxus cerebral vesicle and the developing vertebrate telencephalon(Benito-Gutiérrez et al., 2021). These facts indicate that the network Giacomantonio and Goodhill constructed is conserved in the pre-vertebrate chordate and the vertebrate during evolution.

To further confirm the robustness of the model, we generated 128 Boolean function variations based on the network (Figure 1. A) described by Goodhill in 2018(Goodhill, 2018) by using the combination of replacing “AND” with “OR”. With the default operators, 2 point attractors which correspond to the expression pattern of the posterior (boole_p1) or anterior (boole_p2) telencephalon separately and 2 linear attractors (boole_li7 and boole_li18) were generated by traversing all initial vectors (Figure 1. B). For all Boolean variations, we obtained 26 attractors with 4 point ones and 22 linear ones (Figure 1. B). Among them, two attractors, the

posterior-like attractor boole_p1 and the anterior-like attractor boole_p2, were obtained in all Boolean variations (Figure 1. E). The size of the attraction basins with each attractor in all variations, in which the proportions of boole_p1 and boole_p2 were equivalently the most common with more than 36 % (Figure 1. C, D, E). These results further confirmed the robustness of the Boolean dynamic behavior of this network.

Bifurcations observed with evolving Hill coefficient

Complex dynamic behavior, like transition states and bifurcation, cannot be obtained in Boolean dynamics(P. Ao et al., 2010; Toulouse et al., 2005; Yuan et al., 2017). Thus, we turn our attention to the ordinary differential equation (ODE) model. In this work, we used a double-normalized Hill equation which has been described in detail previously(Toulouse et al., 2005; Yuan et al., 2017). The details of the direct interactions among genes in the current network are still unclear, let alone their dynamic parameters. In order to extract insights from such limited details, a set of dimensionless mesoscopic parameters, h and k, were used in this work.

We chose h=3, k=10 as the first trial of the parameter set (the vanilla set) based on our previous modelling experience(Yuan et al., 2017). Under this set, we obtained three fixed points, with two stable ones (stable state) and an unstable one (transition state) (Figure 2. A, B). The expression patterns of two stable states (Figure 2. A, B; vanilla_sta1, vanilla_sta2) consist with the point attractors in Boolean Dynamics (Figure 2. A, B; Boole_p1, Boole_p2), the transition state also consists with the average of all the linear attractors in the Boolean dynamics with the unaltered functions (Figure 2. A, B; Boole_li_allme: the average of Boole_li_7 and Boole_li_18 in Figure 1. B).

In a nonlinear system, bifurcations may occur as parameters change. Oster and Alberch argued that mathematical bifurcations could be an important mechanism behind development and evolution 40 years ago(François, 2012; Oster & Alberch, 1982). We then tried to explore the parameter space in order to find bifurcations.

Fitting an elephant with a wiggling trunk is not our purpose, therefore the number of arbitrary parameters needs to be reduced at first. The number of the arbitrary parameters in this model equals 20 (2n, n = edge number). Given that the details of these dynamical parameters are not clear, and genes in the core network level should be considered equally important, as we argued before(Ping Ao et al., 2008; Yuan et al., 2017), thus we took the same parameters for all edges, therefore reducing the arbitrary parameters number from 20 to 2. Considering the concentration/function of genes already normalized into [0, 1], in order to center the S shape part of the sigmoid function, we let k = 2^h, therefore reducing the number of arbitrary parameters to 1.

Increasing h (h=10, 25; k=2^h) results in two stable states and one transition state, which is similar with the dynamic behavior under the vanilla parameter set (Figure 2. A, B). Since the Hill equation is equivalent to its Boolean from h takes the limit, we expected the dynamic behavior will not change significantly with further increased h.

Then we explored the parameter space with smaller h, and discovered two bifurcations (2<h<2.01; 2.325<h<2.35; k=2^h). When h<2, there's only one stable state, which has a pattern similar with the transition state with the vanilla parameter set. The pattern gradually evolves from the vanilla transition state-like pattern to a vanilla stable state 2-like pattern with increasing h. Passing over the first bifurcation (2<h<2.01), a transition state emerges, which then evolves to a vanilla stable state 1-like pattern (2.01<h<2.325). The second bifurcation (2.325<h<2.35) gives birth to the second stable state (Figure 2. C).

Evolution of the telencephalon anterior-posterior patterning by bifurcations of the network dynamic behavior

Surprisingly, the dynamic behavior of this network is highly consistent with the facts we know about the evolution of telencephalon.

A telencephalon-like structure has been identified recently in amphioxus with a low level of Pax4/6 and a high level of EmxA and EmxB(Benito-Gutiérrez et al., 2021). Only one stable state exists when weak or negative cooperativity among this network (0<h<2.01) with a low level of Pax6 and intermediate-high level of Emx2, which consists with the expression pattern

of the telencephalon-like structure identified in amphioxus. The expression pattern of this solitary stable state gradually evolves to a posterior telencephalon-like pattern with the increasing h.

With a further increased h ($2.01 \leq h \leq 2.325$), the first bifurcation occurs, giving birth to a stable state and a transition state. The expression pattern of the stable state consists with the posterior part of the telencephalon, and the expression pattern of the popping-out transition state is similar with the anterior part of the telencephalon. We don't know which organism would eventually end in development at this stage. Still, in the development of the vertebrate embryonic central nervous system, the telencephalon first appears near the anterior end of prosencephalon(Briscoe & Ragsdale, 2019).

This model results in two stable states consisting with telencephalon anterior-posterior patterning in vertebrates after the second bifurcation ($h \geq 2.35$); and one transition state which shares the similarity in expression pattern with the telencephalon-like structure in amphioxus as well as the sable state when weak or negative cooperativity among this network, reminds us of the biogenetic law(Levit et al., 2022).

We did not observe any significant variation in the dynamic behavior of this network after the second bifurcation ($h \geq 2.35$). On the biological side, no matter how complex the brain evolves, the binary patterning of pallium/subpallium or olfactory bulb/olfactory cortex can always be observed in the vertebrate telencephalon(Briscoe & Ragsdale, 2019).

Predictions

Based on the results above, we can make the following predictions:

1. The topological structure of the core endogenous network that determines the telencephalon anterior-posterior patterning has already evolved in the ancestral chordate 550 million years ago;
2. The expression pattern of the telencephalon-like structure in such ancestral chordate 550 million years ago and in the Amphioxus today consists with the stable states we obtained before the first bifurcation ($0<h\leq 2$)；
3. An ancestral organism with primitive telencephalon structure would undergo an expression pattern consistent with the anterior part of the vertebrate telencephalon and the transition state we obtained under the parameter range of $2.01\leq h\leq 2.325$ during development, then matured in the expression pattern consistent with the posterior part of the vertebrate telencephalon and the stable state we obtained under this parameter range of $2.01\leq h\leq 2.325$.
4. Experiments that reduce the cooperative effect in the network described above in vertebrates, series of events: the vanishing of the anterior-posterior patterning of the telencephalon; a structure with the expression pattern consists with the posterior part of the telencephalon; a structure with the expression pattern consists with the Amphioxus telencephalon-like structure would be observed.

Conclusion

The current results display such a picture:

The ancestral chordate 550 million years ago evolved a 5-node core endogenous network described in this work with weak or even negative cooperative effect, which determines a telencephalon-like structure with a similar expression pattern with the developing telencephalon during early embryonic stage in the vertebrate, but without the anterior-posterior patterning;

Between 550 million to 500 million years ago, new genes emerged from the genome duplication and mutations. As a result, the cooperative effect in the 5-node core endogenous network increased so that a primitive telencephalon structure gradually evolved to the expression pattern of the posterior part of the vertebrate telencephalon, and during development, it would undergo an expression pattern similar to the anterior part of the vertebrate telencephalon;

With the further increase of the cooperative effect during evolution, a telencephalon with the anterior-posterior patterning emerged, which like the biogenetic law concluded, would undergo a development stage with an expression pattern similar to that of the ancestral telencephalon-like structure.

In a way, we have drawn an answer to how did the telencephalon anterior-posterior patterning evolve quantitively in a first principle manner.

Discussion

For the evolution of the telencephalon anterior-posterior patterning, we found that such a 5-node network alone is sufficient to draw an answer, but it is not enough for the evolution of the whole central nervous system, let alone the entire vertebrate body plan. The network described in this work can be taken as a subnetwork(Wang et al., 2018), which has the potential to expand into the global decision-making network for the evolution and development of the central nervous system or even the entire vertebrate body plan shaped by evolution.

Preliminary evidence suggest the hypothesis that the network described in this work is conserved during evolution from pre-vertebrate chordate to vertebrate is acceptable, the results obtained by Giacomantonio and Goodhill(Giacomantonio & Goodhill, 2010, 2014) and the results described in this work combined further validated this hypothesis at the computational level. Nonetheless, the efforts on the experiments' side to validate the hypothesis are still indispensable.

As the knowledge of the real dynamics parameters is little, if not none, we used a set of dimensionless mesoscopic parameters and made the parameter sets equal at the core network level based on a set of working hypotheses postulated before(Ping Ao et al., 2008; Yuan et al., 2017). This work showed that useful predictions can still be drawn even with such little knowledge. But exploring the range of these parameters in real biological systems is still a non-negligible task.

In response to the growing emphasis on theory-experiment coupling in life science recently(Ping Ao, 2021; MacArthur, 2023; Nurse, 2021; Prokop, 2022; Smaldino, 2019), our work showed that the combination of existing experimental facts as well as the aforementioned mathematical and theoretical framework, although not perfect yet, has been able to give birth to new knowledge and verifiable predictions.

Methods

Boolean dynamics

For the unaltered function set, we used “AND” to represent the interaction of activation, “NOT” to represent the interaction of inhibition:

A=Fgf8 A (t+1) = D (t)

B=Emx2 B (t+1) = NOT A (t)

C=Pax6 C (t+1) = A (t) AND (NOT B (t)) AND (NOT E (t))

D=Sp8 D (t+1) = (NOT B (t)) AND (NOT E (t))

E=Coup-tfi E (t+1) = (NOT A (t)) AND (NOT C(t)) AND (NOT D (t))

For the variants, an agent affected by n agents will result 2^n equations. Thus, we generated 1*1*8*2*8=128 sets of functions. All variants are presented in the supplementary material.

We iterated the function set with traversed initial vectors until stable, then collected and counted attractors, attractor types, and basin of attraction sizes. These data are presented in the supplementary material in detail.

ODE

The ODE functions we used are as follows:

x(1)=Fgf8; $\frac{dx(1)}{dt} = -x(1) + \frac{k*x(5)^h}{1+k*x(5)^h}$

x(2)=Pax6; $\frac{dx(2)}{dt} = -x(2) + \frac{k*x(1)^h}{1+k*x(1)^h} * \frac{1}{1+k*\left(x(3)^h+x(4)^h\right)}$

x(3)=Emx2; $\frac{dx(3)}{dt} = -x(3) + \frac{1}{1+k*x(1)^h}$

x(4)=Coup-tfi; $\frac{dx(4)}{dt} = -x(4) + \frac{1}{1+k*\left(x(1)^h+x(2)^h+x(5)^h\right)}$

x(5)=Sp8; $\frac{dx(5)}{dt} = -x(5) + \frac{1}{1+k*\left(x(3)^h+x(4)^h\right)}$

We used Newton's iteration to obtain fixed points; determined the stability of the fixed point by the real part of the eigenvalue of its Jacobian matrix; used Euler's method to verify the stable fixed points parallelly.

For the vanilla parameter set (n=3, k=10), we first used 1000 random initial vectors, followed by 100000 random initial vectors to verify the integrity of the results. The results showed that

1000 random initial vectors were sufficient to obtain complete results, so 1000 random initial vectors were used to explore the parameter space.

The connection between transition states and stable states was obtained by perturbation on the transition state with a small random vector; in this work, the number of such small random vectors is 100.

Figure 1. Boolean dynamics of the core endogenous network for telencephalon anterior-posterior patterning. A, The network we used in this work. B, Results of Boolean dynamics, linear attractors were averaged. C, The occurrence of attractors among all Boolean equation variations. D, Total size of an attractor in all attractors combined. E, An overview of the attractors for all Boolean variations. The color of the circle represents the attractor type (red: linear attractor; blue: point attractor). Aera of the circle represents the attractor size. Each attractor of each Boolean variant shows the same transparency, thus less transparency represents higher occurrence. _p: point attractor; _l: linear attractor.

Figure 2. A, A Numeric way of showing the bifurcation. All fixed points under all parameter h we have been tried were displayed in this picture, the first column on the left is under vanilla parameter set (h=3, k=10), the rightest column is the results of the unaltered Boolean functions ($h \rightarrow +\infty$), and others are arranged from small to large for h. B, Heatmap of all ODE fixed points demonstrated after hierarchical clustering. C, Bifurcations occur with the growth of h. Arrows point to the stable states from the transition state. sta: stable state; tra: transition state

Contribution

Design: Ao, Yao;

Execution: Sun, Yao, Xiong, Su;

Drafting: Yao, Sun, Zhu;

Figure: Yao, Sun, Xiong;

Revising: Sun, Yao, Xiong, Su, Zhang, Zhu, Ao.

Acknowledgements

This study was supported by grants from the National Natural Science Foundation of China (No. 16Z103060007).

We thank Prof. Wan in the College of Life Sciences, Inner Mongolia Agricultural University for the discussion, Dr. Tang in the Institute of Neurology, Chinese Academy of Sciences and his wife for the inspiration.

We thank Shanghai Nanobubble Technology Co., LTD. for their assistance in publishing this article.

Reference

Ao, P. (2005). Laws in Darwinian evolutionary theory. *Physics of Life Reviews*, *2*(2), 117–156. https://doi.org/10.1016/j.plrev.2005.03.002

Ao, P., Galas, D., Hood, L., Yin, L., & Zhu, X. M. (2010). Towards predictive stochastic dynamical modeling of cancer genesis and progression. *Interdisciplinary Sciences: Computational Life Sciences*, *2*(2), 140–144. https://doi.org/10.1007/s12539-010-0072-3

Ao, Ping. (2021). Towards predictive neural network dynamical theory. *Physics of Life Reviews*, *36*, 30–32. https://doi.org/10.1016/j.plrev.2020.08.006

Ao, Ping, Galas, D., Hood, L., & Zhu, X. (2008). Cancer as robust intrinsic state of endogenous molecular-cellular network shaped by evolution. *Medical Hypotheses*, *70*(3), 678–684. https://doi.org/10.1016/j.mehy.2007.03.043

Benito-Gutiérrez, È., Gattoni, G., Stemmer, M., Rohr, S. D., Schuhmacher, L. N., Tang, J., Marconi, A., Jékely, G., & Arendt, D. (2021). The dorsoanterior brain of adult amphioxus shares similarities in expression profile and neuronal composition with the vertebrate telencephalon. *BMC Biology*, *19*(1), 1–19. https://doi.org/10.1186/s12915-021-01045-w

Briscoe, S. D., & Ragsdale, C. W. (2019). Evolution of the Chordate Telencephalon. *Current Biology*, *29*(13), R647–R662. https://doi.org/10.1016/j.cub.2019.05.026

Chakraborty, M., & Jarvis, E. D. (2015). Brain evolution by brain pathway duplication. *Philosophical Transactions of the Royal Society B: Biological Sciences*, *370*(1684). https://doi.org/10.1098/rstb.2015.0056

François, P. (2012). Evolution in silico: from network structure to bifurcation theory. In *Advances in experimental medicine and biology* (Vol. 751, pp. 157–182). https://doi.org/10.1007/978-1-4614-3567-9_8

Giacomantonio, C. E., & Goodhill, G. J. (2010). A boolean model of the gene regulatory network underlying mammalian cortical area development. *PLoS Computational Biology*, *6*(9). https://doi.org/10.1371/journal.pcbi.1000936

Giacomantonio, C. E., & Goodhill, G. J. (2014). A computational model of the effect of gene misexpression on the development of cortical areas. *Biological Cybernetics*, *108*(2), 203–221. https://doi.org/10.1007/s00422-014-0590-x

Gil-Gálvez, A., Jiménez-Gancedo, S., Pérez-Posada, A., Franke, M., Acemel, R. D., Lin, C.-Y. Y., Chou, C., Su, Y.-H. H., Yu, J.-K. K., Bertrand, S., Schubert, M., Escrivá, H., Tena, J. J., & Gómez-Skarmeta, J. L. (2022). Gain of gene regulatory network interconnectivity at the origin of vertebrates. *Proceedings of the National Academy of Sciences*, *119*(11), 1–12. https://doi.org/10.1073/pnas.2114802119

Goodhill, G. J. (2018). Theoretical Models of Neural Development. *IScience*, *8*, 183–199. https://doi.org/10.1016/j.isci.2018.09.017

Holland, L. Z. (2015). The origin and evolution of chordate nervous systems. *Philosophical Transactions of the Royal Society B: Biological Sciences*, *370*(1684). https://doi.org/10.1098/rstb.2015.0048

Hood, L. (2003). Systems biology: Integrating technology, biology, and computation. *Mechanisms of Ageing and Development*, *124*(1), 9–16. https://doi.org/10.1016/S0047-6374(02)00164-1

Kaessmann, H. (2010). Origins, evolution, and phenotypic impact of new genes. *Genome Research*, *20*(10), 1313–1326. https://doi.org/10.1101/gr.101386.109

Kauffman, S. A. (1969). Metabolic stability and epigenesis in randomly constructed genetic nets.

Journal of Theoretical Biology, *22*(3), 437–467. https://doi.org/10.1016/0022-5193(69)90015-0

Kwon, C., Ao, P., & Thouless, D. J. (2005). *Structure of stochastic dynamics near fixed points*. *102*(37), 13029–13033. https://doi.org/10.1073/pnas.0506347102

Levit, G. S., Hoßfeld, U., Naumann, B., Lukas, P., & Olsson, L. (2022). The biogenetic law and the Gastraea theory: From Ernst Haeckel's discoveries to contemporary views. *Journal of Experimental Zoology Part B: Molecular and Developmental Evolution*, *338*(1–2), 13–27. https://doi.org/10.1002/jez.b.23039

MacArthur, B. D. (2023). Stem cell biology needs a theory. *Stem Cell Reports*, *18*(1), 3–5. https://doi.org/10.1016/j.stemcr.2022.11.005

Marlétaz, F., Firbas, P. N., Maeso, I., Tena, J. J., Bogdanovic, O., Perry, M., Wyatt, C. D. R., de la Calle-Mustienes, E., Bertrand, S., Burguera, D., Acemel, R. D., van Heeringen, S. J., Naranjo, S., Herrera-Ubeda, C., Skvortsova, K., Jimenez-Gancedo, S., Aldea, D., Marquez, Y., Buono, L., … Irimia, M. (2018). Amphioxus functional genomics and the origins of vertebrate gene regulation. *Nature*, *564*(7734), 64–70. https://doi.org/10.1038/s41586-018-0734-6

Nurse, P. (2021). Biology must generate ideas as well as data. *Nature*, *597*(7876), 305–305. https://doi.org/10.1038/d41586-021-02480-z

Oster, G., & Alberch, P. (1982). Evolution and Bifurcation of Developmental Programs. *Evolution*, *36*(3), 444. https://doi.org/10.2307/2408093

Prokop, A. (2022). Towards the first principles in biology and cancer: New vistas in computational systems biology of cancer. *Life*, *12*(1). https://doi.org/10.3390/life12010021

Putnam, N. H., Butts, T., Ferrier, D. E. K., Furlong, R. F., Hellsten, U., Kawashima, T., Robinson-Rechavi, M., Shoguchi, E., Terry, A., Yu, K., Benito-Gutiérrez, È., Dubchak, I., Garcia-Fernàndez, J., Gibson-Brown, J. J., Grigoriev, I. V., Horton, A. C., De Jong, P. J., Jurka, J., Kapitonov, V. V., … Rokhsar, D. S. (2008). The amphioxus genome and the evolution of the chordate karyotype. *Nature*, *453*(7198), 1064–1071. https://doi.org/10.1038/nature06967

Smaldino, P. (2019). Better methods can't make up for mediocre theory. *Nature*, *575*(7781), 9–9. https://doi.org/10.1038/d41586-019-03350-5

Takatori, N., Butts, T., Candiani, S., Pestarino, M., Ferrier, D. E. K., Saiga, H., & Holland, P. W. H. (2008). Comprehensive survey and classification of homeobox genes in the genome of amphioxus, Branchiostoma floridae. *Development Genes and Evolution*, *218*(11–12), 579–590. https://doi.org/10.1007/s00427-008-0245-9

Toulouse, T., Ao, P., Shmulevich, I., & Kauffman, S. (2005). Noise in a small genetic circuit that undergoes bifurcation. *Complexity*, *11*(1), 45–51. https://doi.org/10.1002/cplx.20099

Wang, G., Yuan, R., Zhu, X., & Ao, P. (2018). *Endogenous Molecular-Cellular Network Cancer Theory: A Systems Biology Approach* (Vol. 1702, pp. 215–245). https://doi.org/10.1007/978-1-4939-7456-6_11

Weinberg, R. A. (2014). Coming full circle - From endless complexity to simplicity and back again. *Cell*, *157*(1), 267–271. https://doi.org/10.1016/j.cell.2014.03.004

Yuan, R., Zhu, X., Wang, G., Li, S., & Ao, P. (2017). Cancer as robust intrinsic state shaped by evolution: a key issues review. *Reports on Progress in Physics*, *80*(4), 042701. https://doi.org/10.1088/1361-6633/aa538e

ZHU, X.-M., YIN, L., HOOD, L., & AO, P. (2004). ROBUSTNESS, STABILITY AND EFFICIENCY OF PHAGE λ GENETIC SWITCH: DYNAMICAL STRUCTURE ANALYSIS. *Journal of Bioinformatics and Computational Biology*, *02*(04), 785–817.

https://doi.org/10.1142/S0219720004000946

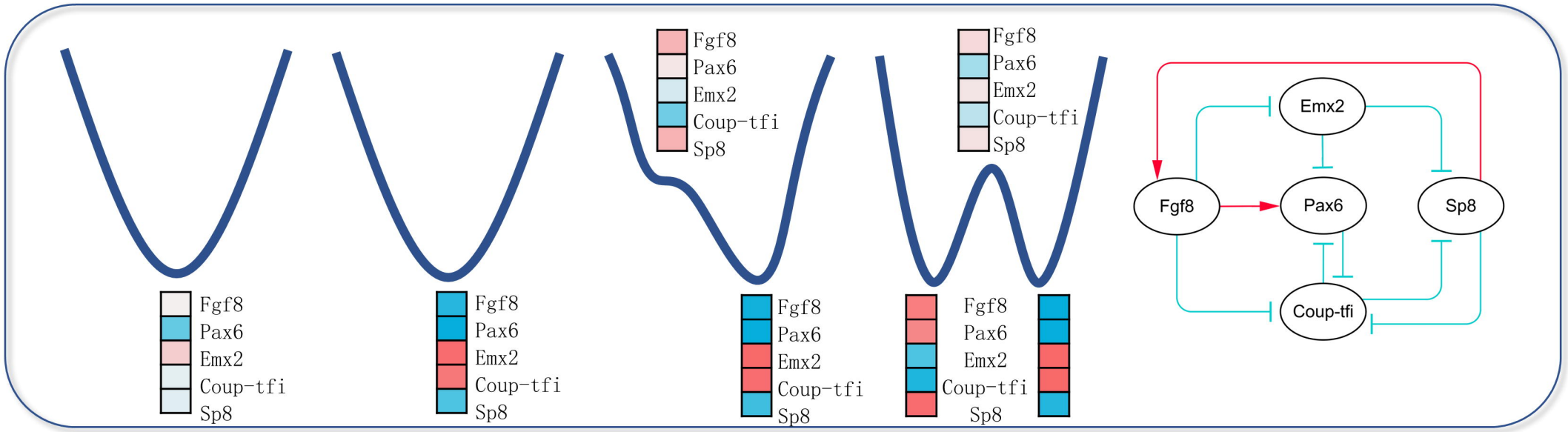
Fgf8
Pax6
Emx2
Coup-tfi
Sp8
Fgf8
Pax6
Emx2
Coup-tfi
Sp8
Fgf8
Pax6
Emx2
Coup-tfi
Sp8
Fgf8
Pax6
Emx2
Coup-tfi
Sp8
Fgf8
Pax6
Emx2
Coup-tfi
Sp8
Fgf8
Pax6
Emx2
Coup-tfi
Sp8
Fgf8
Pax6
Emx2
Coup-tfi
Sp8
Fgf8
Pax6
Emx2
Coup-tfi
Sp8
Fgf8
Pax6
Emx2
Coup-tfi
Sp8

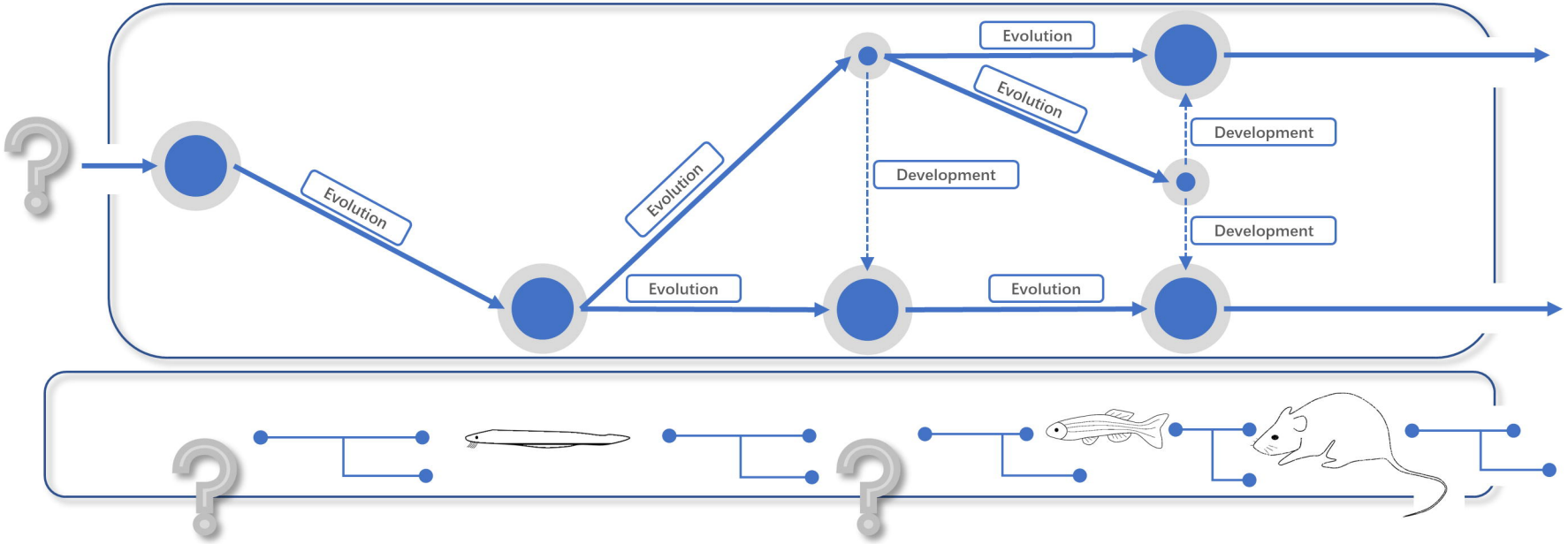
Evolution
Evolution
Evolution
Evolution
Evolution
Evolution
Development
Development
Development

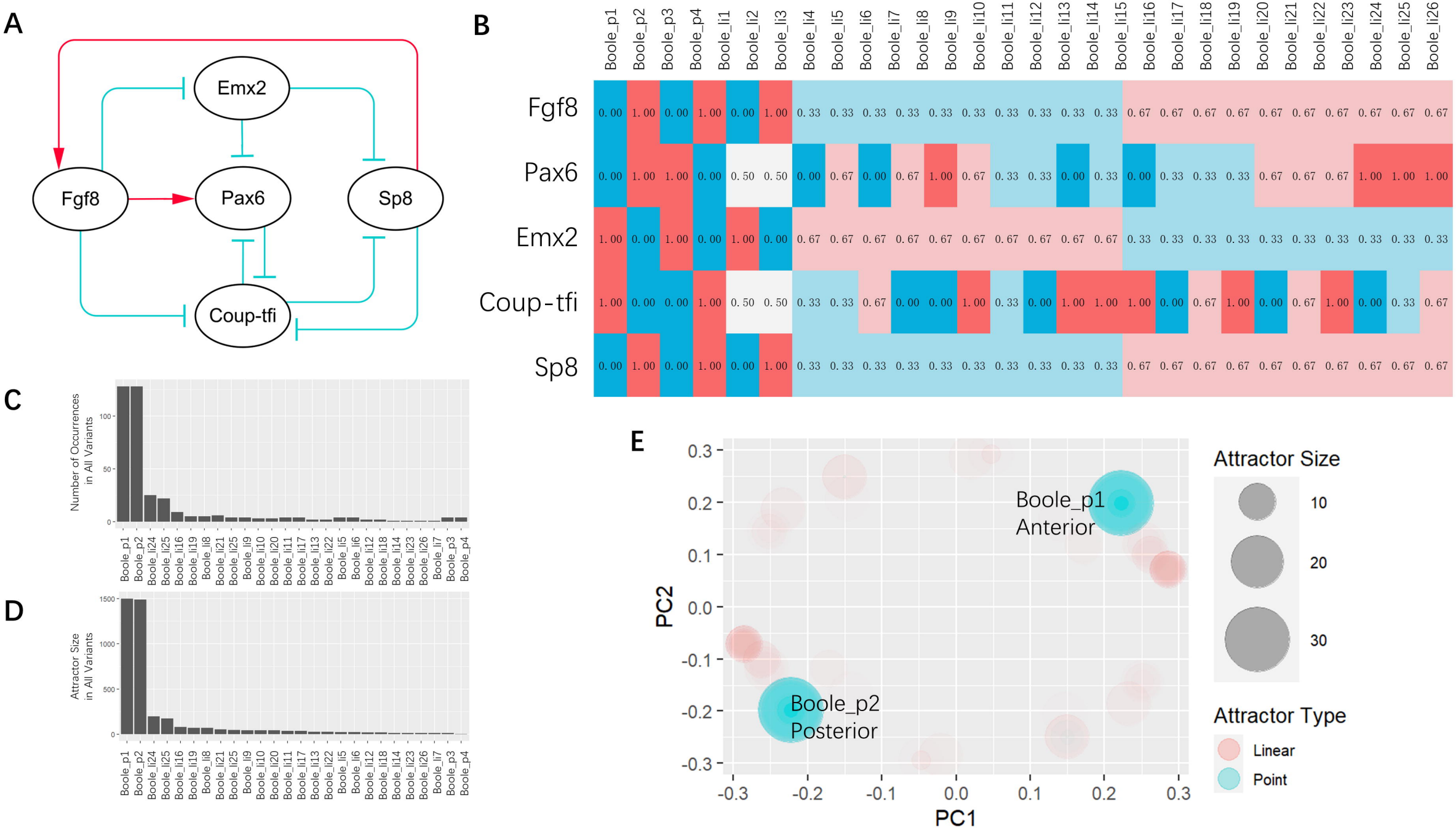
A
Emx2
Fgf8
Pax6
Sp8
Coup-tfi
B
Boole_p1 Boole_p2 Boole_p3 Boole_p4 Boole_li1 Boole_li2 Boole_li3 Boole_li4 Boole_li5 Boole_li6 Boole_li7 Boole_li8 Boole_li9 Boole_li10 Boole_li11 Boole_li12 Boole_li13 Boole_li14 Boole_li15 Boole_li16 Boole_li17 Boole_li18 Boole_li19 Boole_li20 Boole_li21 Boole_li22 Boole_li23 Boole_li24 Boole_li25 Boole_li26
Fgf8 0.00 1.00 0.00 1.00 0.00 1.00 0.33 0.33 0.33 0.33 0.33 0.33 0.33 0.33 0.33 0.33 0.67 0.67 0.67 0.67 0.67 0.67 0.67 0.67 0.67 0.67
Pax6 0.00 1.00 1.00 0.00 0.50 0.50 0.00 0.67 0.00 0.67 1.00 0.67 0.33 0.33 0.00 0.33 0.00 0.33 0.33 0.33 0.67 0.67 0.67 1.00 1.00 1.00
Emx2 1.00 0.00 1.00 0.00 1.00 0.00 0.67 0.67 0.67 0.67 0.67 0.67 0.67 0.67 0.67 0.67 0.33 0.33 0.33 0.33 0.33 0.33 0.33 0.33 0.33 0.33
Coup-tfi 1.00 0.00 0.00 1.00 0.50 0.50 0.33 0.33 0.67 0.00 0.00 1.00 0.33 0.00 1.00 1.00 1.00 0.00 0.67 1.00 0.00 0.67 1.00 0.00 0.33 0.67
Sp8 0.00 1.00 0.00 1.00 0.00 1.00 0.33 0.33 0.33 0.33 0.33 0.33 0.33 0.33 0.33 0.33 0.67 0.67 0.67 0.67 0.67 0.67 0.67 0.67 0.67 0.67
C
Number of Occurrences in All Variants
100
50
0
Boole_p1 Boole_p2 Boole_li24 Boole_li25 Boole_li16 Boole_li19 Boole_li8 Boole_li21 Boole_li25 Boole_li9 Boole_li10 Boole_li20 Boole_li11 Boole_li17 Boole_li13 Boole_li22 Boole_li5 Boole_li6 Boole_li12 Boole_li18 Boole_li14 Boole_li23 Boole_li26 Boole_li7 Boole_p3 Boole_p4
D
Attractor Size in All Variants
1500
1000
500
0
Boole_p1 Boole_p2 Boole_li24 Boole_li25 Boole_li16 Boole_li19 Boole_li8 Boole_li21 Boole_li25 Boole_li9 Boole_li10 Boole_li20 Boole_li11 Boole_li17 Boole_li13 Boole_li22 Boole_li5 Boole_li6 Boole_li12 Boole_li18 Boole_li14 Boole_li23 Boole_li26 Boole_li7 Boole_p3 Boole_p4
E
PC2
0.3
0.2
0.1
0.0
-0.1
-0.2
-0.3
PC1
-0.3 -0.2 -0.1 0.0 0.1 0.2 0.3
Boole_p1
Anterior
Boole_p2
Posterior
Attractor Size
10
20
30
Attractor Type
Linear
Point

A

	vanilla_sta1	h_1.5_sta1	h_2_sta1	h_2.01_sta1	h_2.325_sta1	h_2.35_sta1	h_2.5_sta1	h_2.75_sta1	h_3_sta1	h_10_sta1	h_25_sta1	Boole_p1
Fgf8	0.00	0.27	0.05	0.05	0.02	0.02	0.01	0.00	0.00	0.00	0.00	0.00
Pax6	0.00	0.08	0.00	0.00	0.00	0.00	0.00	0.00	0.00	0.00	0.00	0.00
Emx2	1.00	0.71	0.99	0.99	1.00	1.00	1.00	1.00	1.00	1.00	1.00	1.00
Coup-tfi	1.00	0.54	0.94	0.94	0.98	0.98	0.99	1.00	1.00	1.00	1.00	1.00
Sp8	0.05	0.26	0.12	0.12	0.09	0.09	0.08	0.07	0.06	0.00	0.00	0.00

	vanilla_tra1	h_0.1_sta1	h_0.5_sta1	h_1_sta1	h_1.1_sta1	h_2.35_tra1	h_2.5_tra1	h_2.75_tra1	h_3_tra1	h_10_tra1	h_25_tra1	Boole_li_allme
Fgf8	0.50	0.49	0.46	0.42	0.41	0.64	0.58	0.55	0.53	0.50	0.50	0.50
Pax6	0.25	0.17	0.18	0.16	0.16	0.41	0.34	0.30	0.29	0.25	0.25	0.17
Emx2	0.45	0.50	0.51	0.54	0.56	0.36	0.41	0.44	0.45	0.50	0.50	0.50
Coup-tfi	0.30	0.26	0.29	0.35	0.36	0.19	0.24	0.27	0.28	0.33	0.33	0.17
Sp8	0.46	0.34	0.36	0.36	0.35	0.64	0.57	0.54	0.52	0.50	0.50	0.50

	vanilla_sta2	h_2.01_tra1	h_2.325_tra1	h_2.35_sta2	h_2.5_sta2	h_2.75_sta2	h_3_sta2	h_10_sta2	h_25_sta2	Boole_p2
Fgf8	0.90	0.62	0.67	0.70	0.79	0.85	0.88	1.00	1.00	1.00
Pax6	0.87	0.33	0.45	0.50	0.64	0.75	0.82	1.00	1.00	1.00
Emx2	0.12	0.36	0.34	0.31	0.24	0.19	0.16	0.00	0.00	0.00
Coup-tfi	0.04	0.18	0.17	0.15	0.10	0.07	0.06	0.00	0.00	0.00
Sp8	0.98	0.57	0.67	0.72	0.84	0.93	0.97	1.00	1.00	1.00

B

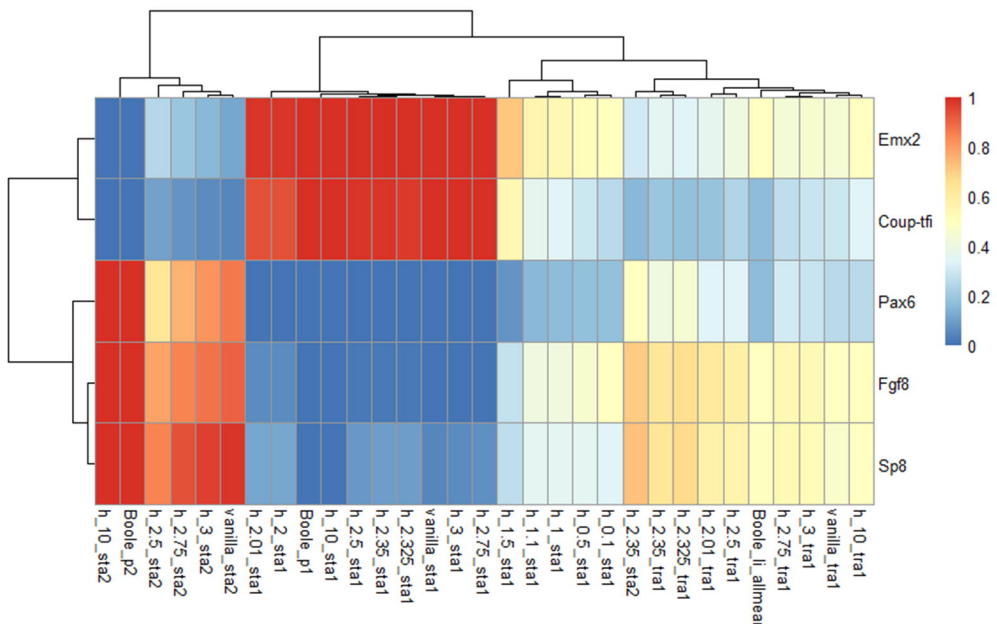
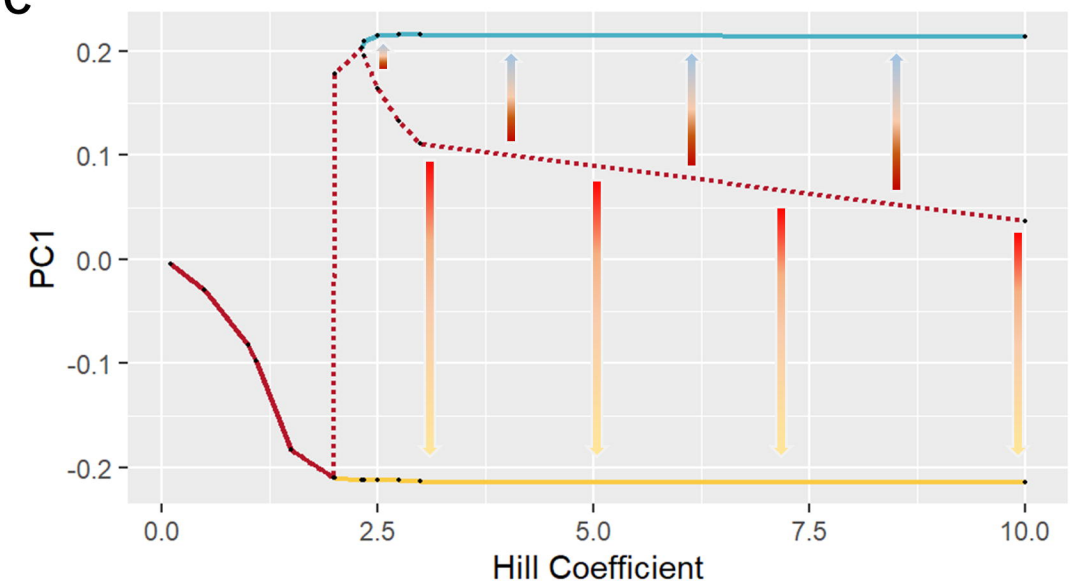
C